Structure and Property Relationships of Amorphous CN_x: A Joint Experimental and Theoretical Study

M.C. dos Santos and F. Alvarez

Instituto de Física "Gleb Wataghin", Universidade Estadual de Campinas

Caixa Postal 6165, 13083-970, Campinas, São Paulo, Brazil

Received 30 November, 2000

Amorphous CN_x and CN_x:H have been prepared by the ion beam assisted deposition technique. Samples were characterized through X-ray and UV photoemission, IR absorption and Raman spectroscopies. These spectra have been interpreted with the aid of quantum chemical calculations based upon the Hartree-Fock theory on several molecular models. The understanding of the electronic and structural properties of the amorphous alloy as a function of nitrogen content could help in the task of synthesizing the metastable silicon-nitride like-phase β-C_3N_4, a solid which has been predicted to be as hard as diamond. The physical picture emerging from the present study helps to clarify the difficulties in obtaining the crystalline phase of the material, suggesting new experimental directions for syntheses.

I Introduction

The interest on carbon nitride materials was raised in early 1920's [1], when it was suggested that the solid C_3N_4 might exist in a graphitic form. However, the search for this material started much later, at the end of the 1980's, after Liu and Cohen [2] predicted the existence of a metastable fully covalent carbon nitride (β-C_3N_4) having the same structure of the known compound Si_3N_4. This theoretical prediction was based on *ab initio* calculations which suggested for the first time the possible existence of a material as hard, or even harder, than diamond. In addition, the authors demonstrated in this article the powerfulness of modern electronic structure techniques in predicting new structures and properties of solids.

Considerable interest was devoted to carbon-nitrogen alloys since then. Although serious problems have emerged to produce the predicted crystalline phase, amorphous CN_x films exhibit useful optical and mechanical properties [3]. Recent experiments show that CN_x alloys undergo profound structural changes upon the variation of the nitrogen concentration. Increasing the amount of N up to ~20 at. % notably augment the hardness and elasticity of the material [4]. Recently, a super hard C-N alloy with hardness as high as 40-60 Gpa was reported [5,6]. Besides the obvious technological potentiality, the alloy is an interesting system *per se* for basic studies. For instance, theoretical calculations predict the existence of closed molecular structures such as fullerene-like and tubular carbon nitrides [7]. Indeed, nanotubes formed in some non- stoichiometric C-N alloys were attributed to be the cause of the surprising hardness of the material [5]. Techniques to produce carbon nitride tubulites are currently being developed [8,9].

In spite of the large amount of studies already performed, the complexity of the structure of carbon-nitrogen materials has prevented a clear understanding of several basic aspects of the alloy. In this paper we present theoretical calculations and experimental results regarding the study of this interesting material. Carbon nitride thin films were prepared with varying N content. The local structure and the top of the valence band as function of the nitrogen concentration is reported. The role of N bending and buckling the structure towards the formation of molecular forms is discussed and the influence of hydrogen in the properties of carbon-nitrogen alloy is also reported. The vibrational spectrum of the amorphous material is investigated through Raman and infra-red spectroscopies in combination with isotopic ^{15}N and D substitution. Molecular models were adopted to theoretically investigate the roles of nitrogen binding to carbon as well as the isotopic shift on the vibrational spectra. This paper is organized as follows: a brief presentation of the theory adopted is made in section II, together with the main results; section III gives the experimental details on sample preparation and characterization. Results

and the interpretation made with the aid of theoretical models is presented in section IV. The last section is devoted to conclusions.

II Theory

The theoretical approach relies on calculations of density of states (DOS) and core level binding energies of model molecules containing C and N. The starting point of all calculations is the determination of the ground state molecular conformation. Geometry optimizations of the molecular structures and the vibrational analysis were performed based on the semi-empirical Austin Method 1 (AM1) and Parametric Model 3 (PM3) [10] quantum chemical techniques. Only the clusters related to C_3N_4, taken from the predicted crystal structure, were not optimized.

II.1. Core-level binding energy

Small molecules representative of the chemical bond in C-N alloys are chosen for evaluation of the chemical shifts on the N1s electron binding energy [11]. The electronic structures of the optimized molecular conformations was obtained through *ab initio* 6-31G** calculations [12]. The molecules include sp, sp^2 and sp^3 carbon and nitrogen hybridizations and fragments of the theoretically predicted α and β carbon-nitride (C_3N_4) compound [2,13]. The numerical values associated to each structure are grouped as follows: a) sp^3 N bonded to sp^3 C in "open" structures; b) sp^2 N substituting sp^2 carbon in aromatic structures; c) sp N in nitrile compounds and sp^2 N in pyridine; d) sp^3 N bonded to sp^3 C in a closed structure in which C-N-C bonds are stressed. These calculations found four typical values of binding energies: (a) ~398.3-398.6 eV for threefold coordinated N bonded to fourfold coordinated C, (b) ~401.9-401.0 eV for substitutional sp^2 N in graphite-like structures; (c) ~399.2 eV for sp^2 N (pyridine-like) or ~399.4 eV for sp N; and (d) ~399.0 eV for a stressed structure containing sp^3 N.

II.2. Valence-band electronic structure

Large clusters including up to 96 carbon atoms in the graphite symmetry were adopted to study the valence band (VB) electronic structure by randomly replacing C with N atoms [11]. The electronic structure was obtained by the Valence Effective Hamiltonian (VEH) method [14]. Bonds at the boundary were saturated with hydrogen. Systems containing [N]/[C] = 0,7%, 14%, 20%, 23%, 37% and 100% were studied. Two main sets were optimized: 1) one set imposing C_s symmetry to maintain planar geometry; and 2) a second set allowing full relaxation of the atomic coordinates. As before, the electronic structures of the optimized molecules were obtained by the VEH Method. A cluster representing β-C_3N_4 has been taken from the predicted crystal structure, containing 36 C and 48 N atoms, with end bonds saturated with hydrogen, and the DOS was calculated. For comparison purposes, the Fermi energy of the pure graphite cluster was shifted to zero. Histograms were obtained by the usual counting of states procedure. The DOS were normalized for comparison purposes, since the clusters may have different number of atoms [7,11].

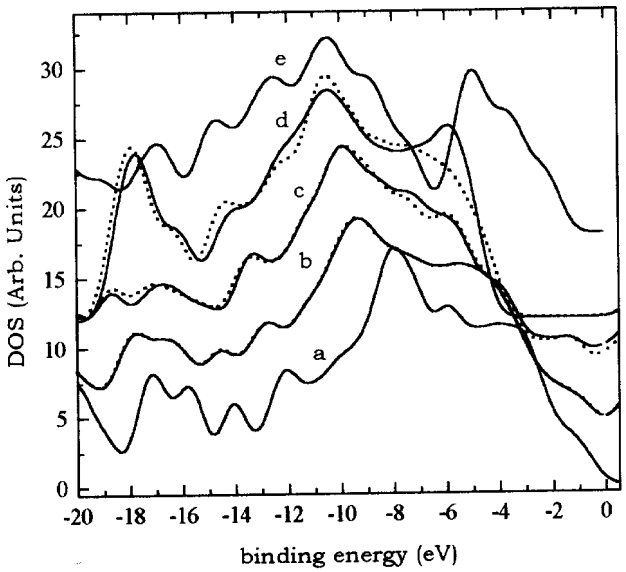

Figure 1. Simulated densities of states of carbon-nitrogen clusters from VEH calculations, for a graphite, b [N]/[C] = 14%, c [N]/[C] = 37%, d [N]/[C] = 100%, and e C_3N_4 cluster. Plots were shifted upward for better visualization.

Fig. 1 displays the simulated densities of states of graphite (curve a), N-substituted graphite at the concentrations [N]/[C] = 14% (curves b), 37% (curves c), and 100% (curves d), and the DOS of the β-C_3N_4 cluster (curve e). The plots are shifted upward for better visualization. The curves b, c, and d are plotted in pairs, representing the DOS of planar (dotted) and fully optimized (continuous) N-substituted graphite clusters. In a the wide feature at ~ 3.0 eV, due to electrons coming from the π bonds, and at ~ 8.0 eV, due to σ bonds, are clearly seen. These peaks are shifted to higher binding energies as more and more nitrogen atoms replace carbons in the cluster. At [N]/[C] = 14%, curves b, differences between the DOS are negligible since the fully optimized cluster remains planar. Differences are fully developed at [N]/[C] =100%: while the graphite-like system presents a DOS profile similar to that of graphite, shifted to higher binding energies, the structure of the fully optimized cluster is distorted and the buckling results in two well defined peaks in the corresponding DOS, at ~ 11.0 eV and ~ 6.0 eV, the latter

originating from nitrogen lone-pairs. The last DOS, curve e, presents two features located at ~11.0 eV and 5.0 eV and are due to electrons coming from C-N σ bonds and N lone-pairs, respectively, of the β-C_3N_4 structure.

II.3. Vibrational structure

We have performed calculations of the frequencies and intensities of the infra-red active vibrations of several organic molecules. These calculations are aimed at investigating the roles of symmetry breaking effects of substitutional N on graphite structure and isotopic shifts due to ^{15}N. Firstly, we obtained the spectra of the small molecules schematically shown in Fig. 2. Molecule M1 is an aromatic molecular radical having D_{3h} symmetry. Substitution of the central carbon atom by N, as in molecule M2, is intended to investigate the effects due to charge rearrangement while in M3 molecule the substitution site reduces the symmetry to C_{2v}.

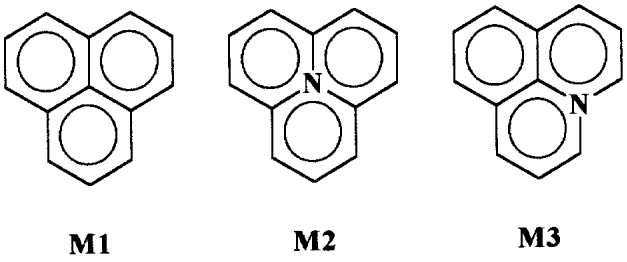

Figure 2. Molecular models adopted in PM3 calculations of IR spectra.

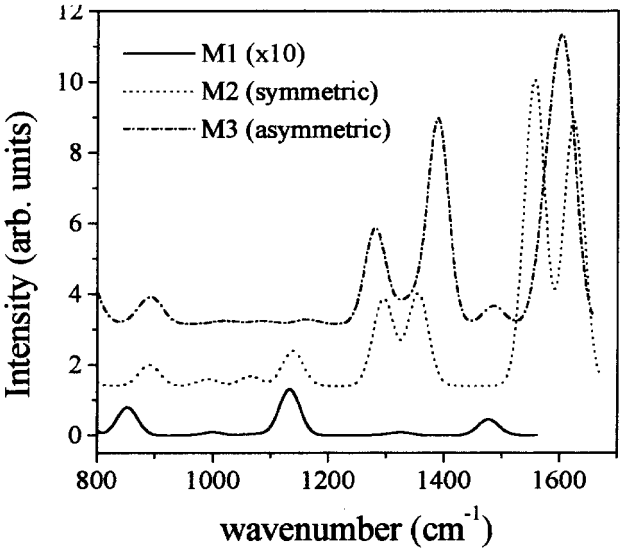

Figure 3. Simulated PM3 IR-active vibration spectra of the model molecules M1(continuous line, scaled by 10), M2 (dotted) and M3 (dash-dotted). The curves were translated upward for clarity.

The molecular conformations were optimized and the vibration analysis was performed. Fig. 3 depicts the simulated spectra in the region 800-1600 cm^{-1} evaluated as gaussian convolutions of the calculated intensities. The gaussian broadening was arbitrarily taken as 20 cm^{-1}.

Molecule M1 is very homogeneous in charge distribution and in C-C bond lengths, resulting in very low ir intensities in the stretching region, as expected. Notice that the curve in Fig. 2 corresponding to M1 has been scaled by a factor of 10 to allow comparisons with the other spectra. Replacement of the central C atom by N brings a new charge distribution in which second neighbors carbons around N get negative charges through the π system. The consequence is the activation of C-C stretching vibrations, as seen in Fig. 3, in the region 1200-1600 cm^{-1}. These collective vibrations also include the C-N stretching, which shifts the spectrum to higher frequencies, from ~1500 cm^{-1} to 1600 cm^{-1}. There are differences between the spectra of M2 and M3 due to the their particular symmetry group, but the intensities are of the same order of magnitude. This means that the most relevant effect of N substitution in the ir spectrum of the aromatic system is the promotion of bond dipoles.

This result holds for larger systems provided that the aromaticity is preserved. We have performed similar calculations on large graphitic clusters containing up to 96 carbon atoms, as described in the previous subsection. Fig. 4 depicts the simulated spectra for carbon clusters saturated with hydrogen at the end bonds. Two of them were randomly substituted by 6 and 26 nitrogen atoms, respectively. The latter cluster is not planar (see Ref.7). The plot corresponding to C_{96} has been scaled by a factor of 10 and successive plots have been shifted upward for better visualization.

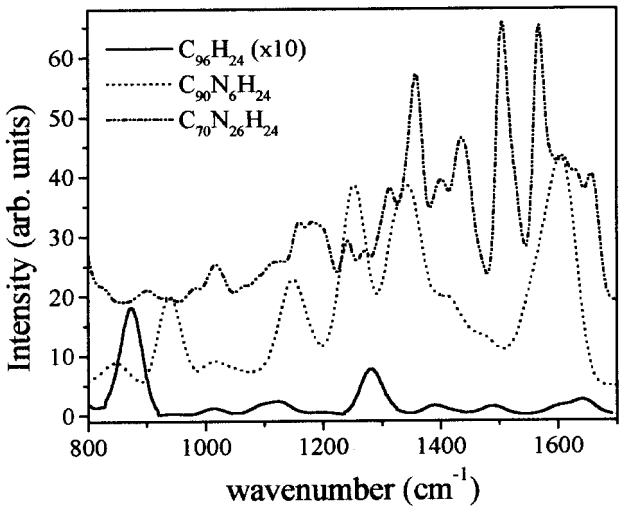

Figure 4. Simulated IR spectra of large carbon clusters from PM3 calculations. The curves were translated upward for clarity. $C_{96}H_{24}$ (continuous line, scaled by 10), $C_{96}N_6H_{24}$ (dotted), $C_{96}N_{26}H_{24}$ (dash-dotted).

These simulated spectra show the same features seen in Fig. 3, namely, weak ir activity of the graphene cluster and the growing of structures in the range 1200-1600 cm^{-1} as nitrogen atoms are incorporated into the aromatic framework. These features are associated to collective C-C and C-N vibrations. The heavily doped cluster $C_{96}N_{26}H_{24}$ is not graphitic. In this disordered system the vibrations are localized in sub-clusters, giving rise to a more intricate spectrum. The vibrations above 1600 cm^{-1} are due to the stretching of C=C bonds at the cluster edges.

Similar calculations were carried out to evaluated the isotopic effects of ^{15}N. We considered simple systems as the aromatic molecules M2 and M3, in which sp^2 hybridized N atoms participate in extensive π bonds; sp and sp^2 N in H_3C-C≡N and H_3C-N=C$(CH_3)_2$ and the large cluster $C_{96}N_{26}H_{24}$, containing sp^3 N. The isotopic shifts of sp and sp^2 N compounds are 27 cm^{-1} and 22 cm^{-1}, respectively. In the aromatic systems the frequency shift is as small as 9 cm^{-1}, because the vibrations in which N atoms participate are collective, thus minimizing the isotope effect. In the large cluster containing sp^3 N several frequencies are shifted by an amount ranging from 2 to ∼15 cm^{-1}, but on the average the shift is below 10 cm^{-1}. The conclusion is that ^{15}N isotopic effect is clearly seen when the associated vibration is *localized.* For instance, -C≡N species that appear in amorphous carbon nitride are expected to act as end groups and the associated vibrations are localized. In this case the C-N stretching vibration should be shifted by ∼30 cm^{-1} upon ^{15}N substitution. In collective vibrations, the isotopic shift could be more difficult to be observed since other effects might produce similar modifications in the ir spectrum.

III Experimental

Two types of samples were prepared: amorphous carbon-nitrogen thin films and graphite powder containing nitrogen. The powder was produced in similar conditions of those used to obtain fullerene [15]. In general, fullerenes are deposited in a conventional bell jar where two high purity graphite electrodes are vaporized by an arc discharge between them. The base pressure of the chamber was ∼ 10^{-4} Pa. In fullerene production, the nucleation is promoted by He [16]. In order to quench the reaction, a suitable atmosphere of N_2 and He at 100-200 mb was used. The residual soot on the chamber was collected and analyzed *ex situ* by mass spectrometry. The a-CN_x:H films were prepared in an Ion Beam Assisted Deposition (IBAD) attached to an Ultra High Vacuum chamber for Photoelectron Spectroscopy Analysis (PES). In IBAD method, a high purity graphite target (99.99 at. %) was sputtered by a N ions beam. Simultaneously a suitable mixture of N, Ar and H ions bombarded the growing film [17]. The relative partial pressures, energies and current density of the sputtering and assisting beams allow the variation of the deposition conditions. In the attempt to elucidate the origin of the IR absorption bands, samples deposited using the isotope $^{15}N_2$ and regular $^{14}N_2$ were grown in nominally identical conditions. To separate the influence of hydrogen and nitrogen, we have studied alloys with and without hydrogen covering the range below and above 20 at. % nitrogen content. The samples were deposited on polished Si wafers (100) and Corning glass a substrate maintained at constant temperature. The base pressure of the chamber was $\sim 2 \times 10^{-5}$ Pa. Immediately after deposition the films were transferred to the UHV chamber ($< 2.0 \times 10^{-9}$ mbar) and measured without further treatment. Some samples were prepared *ex situ* by radio frequency sputtering of a high purity graphite target in a controlled gaseous mixture of Ar and N_2 [11,18]. No important differences were found between these films and those grown by IBAD. On the other hand, hydrogenated samples show profound differences compared to non-hydrogenated samples. As we shall see bellow, hydrogenated samples drastically evolve when exposed to the atmosphere.

The evolution of the binding energies of core level electrons and the top of the valence band on nitrogen incorporation in the samples were analyzed by XPS and UPS, respectively. For the XPS analysis the Al Kα line was used (hν = 1486.6 eV, width 0.85 eV). For UPS the HeI (21.3 eV) and HeII (40.8 eV) lines from a resonant discharge lamp were used. When appropriate, the inelastic background of the spectra was subtracted by standards methods [19]. The total spectrometer resolution was 0.3 eV. After the XPS and UPS experiments, the samples were further analyzed by infra-red (IR), Raman, and visible spectroscopy. The thickness of the samples was measured using a profilometer. The IR and Raman spectra were obtained *ex situ* in a FTIR NICOLET 850 spectrometer and in a Micro-Raman (excitation lines: 520.8 nm and 488 nm from Kr and Ar lasers), respectively. When necessary, nuclear techniques were used to measure hydrogen concentrations [20]. Measurements of stress, conductivity and hardness were also performed.

IV Results

IV.1 Core levels

Fig. 5 shows the experimental evolution of the N1s core level spectra on N concentration. The curves show two well-resolved structures at 398.2 and 400.5 eV (from now on peaks P_1 and P_2) associated with N atoms in two quite different local configurations [11]. Peak P_1 becomes dominant in the material containing high N concentration. This suggests that, depending on the amount of N incorporated in the sample, a particular

structure is favored (curve a, Fig. 5). The *ab initio* simulation shows that the N1s spectra of configurations containing N bonded to C sp^3 (i.e., group a, section II.2) and substitutional N sp^2 (i.e., group b, section II.2) are consistently near to the positions of peaks P_1 and P_2, respectively. Therefore, these results suggest that the coordination of N goes from a planar structure to a three-dimensional structure.

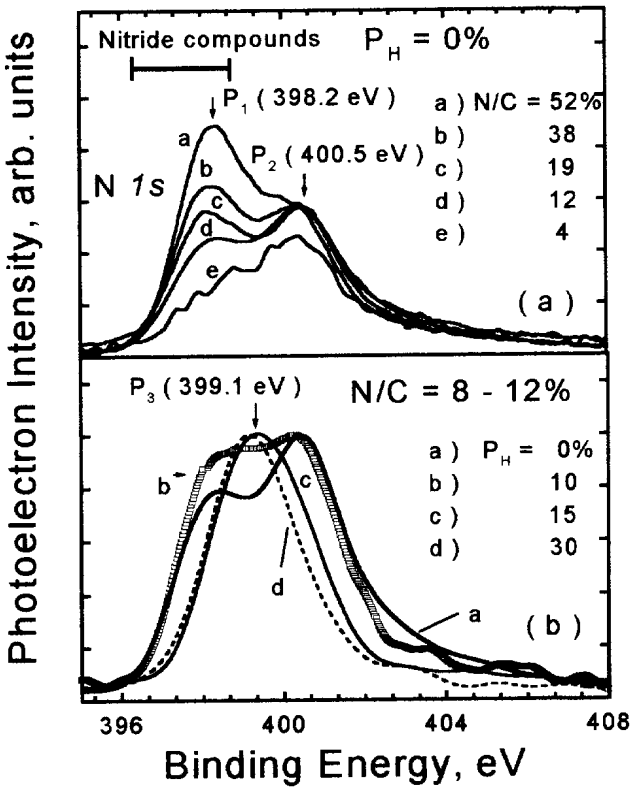

Figura 5. Photoemission spectra of the N1s core-level of the a-CN_x alloy.

IV.2. Valence-band results

Fig. 6 shows the UPS spectra of the studied samples. The spectrum of pure a-C shows two bands located at binding energies ~7.7 eV and ~3.6 eV, respectively. These bands come from σ and π bonds due to C2p electrons. On increasing N content three new features emerge at energies near to ~9.5 eV, ~7.1 eV, and ~4-5 eV, labeled as peaks C, B, and A in Fig. 6. For N/C ratios larger that 20%, the bands at 7.7 eV and 3.6 eV present in pure carbon disappear completely. Also, the band at 7.1 eV dominates the spectrum for films with intermediate N content (10% < N/C < 25%). The bands at ~9.5 eV and ~4-5 eV are wider and increase slowly for larger N/C ratios (>25%). These bands dominate the spectra for the highest nitrogenated samples. Finally, the leading edge of the VB recedes on increasing N content.

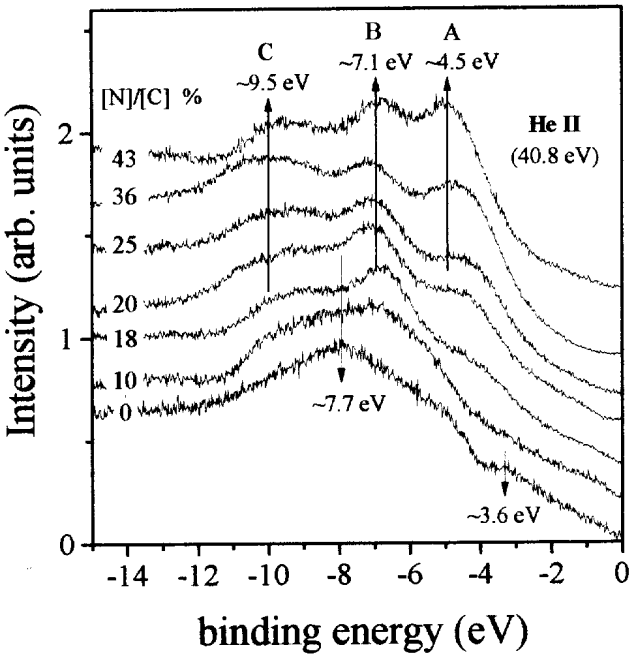

Figura 6. Valence band photoelectron spectra of a-CN_x samples.

A comparison of the experimental curves with the theoretical simulations suggests that peaks A, B and C are due to N lone-pair electrons, π electrons of C-N bonds, and σ electrons of C-N bonds, respectively. Moreover, in order to reproduce the total DOS of samples with N/C > 20% ratio, it is necessary to assume a partial contribution of DOS due to N lone-pair electrons as in the β-C_3N_4 phase (see Figs. 1 and 6). Below N/C ~ 18-20% ratio, the lack of structure at ~4-5 eV in the experimental curves suggests that N is occupying sites in graphite-like structures. Concluding, below the N/C~ 18-20% ratio, N is occupying a C site in graphite-like structures. Above N/C ~ 18-20% ratio, the alloy tends to form a three-dimensional structure with C and N atoms fourfold and threefold coordinated, respectively.

IV.3. Vibrational spectra

Most of the interpretation of the Raman and infrared (IR) spectra of carbon-nitrogen alloys (a-CN_x) relies on the pioneering work of Kaufman et al.[21]. These authors reported no significant changes in the Raman spectra for *hydrogenated* samples containing nitrogen between 0 and ~20 at. %. On the contrary, the IR spectra show profound changes as a function of nitrogen content. The conclusion of this work is that the increasing IR activity stems from the fact that nitrogen breaks the symmetry of the aromatic and/or acetylene groups that constitute the material. Nevertheless there are the above structural data to be considered when analyzing the experimental findings of Kaufman et al..

First, the inclusion of hydrogen profoundly modifies the structure of the alloy [17,20,22]. Second, above ~20 at. % nitrogen content the alloy undergoes a structural change [7,11,23]. The former result is particularly important since in Ref. 21 the changes in the IR spectra are *exclusively* ascribed to nitrogen. In a previous work, we have shown that hydrogen modifies the IR spectra in samples containing similar amounts of nitrogen and different hydrogen contents. In regard to the structural changes introduced by nitrogen, the cited experimental findings prevent to extend *a priori* the results of Kaufman et al. to alloys with nitrogen concentrations above ~20 at. %. Indeed, below this concentration, nitrogen substitution of carbon maintains the planar geometry of graphite, producing a stressed and hard material [23,24]. Above ~20 at. % nitrogen content the graphite sheets curl and a band of localized nitrogen lone pair is formed [7]. The material becomes less dense and -C≡N species are promoted. Therefore, any study should take in consideration these structural differences.

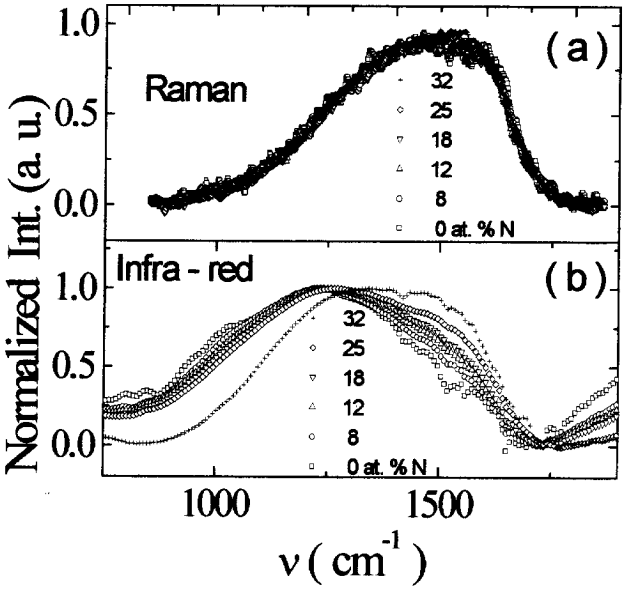

Figure 7. Raman (a) and infrared (b) spectra of *non-hydrogenated* samples.

Fig. 7 shows the normalized Raman (a) and IR (b) spectra of the studied non-hydrogenated samples. As observed, only minor differences are found in the Raman spectra. Although less dramatic than hydrogen [24], nitrogen also increases the I(G) / I(D) intensity ratio of the IR spectra. Here, "G" identifies the band at 1570 cm^{-1} ("graphitic" component) and "D" the band at ~1360 cm^{-1} ("disordered" component) [25]. On increasing amount of nitrogen the similitude of the IR and Raman spectra is evident. We have remarked above that the increasing IR activity is associated with the symmetry breaking of aromatic and/or acetylene groups on nitrogen incorporation. This conclusion relies on the absence of isotopic effect in the ~1000 - 1600 cm^{-1} region of the IR spectra by substitutional 15N2 in hydrogenated samples containing up to ~ at. 20 at. % nitrogen. In the attempt to separate the role of hydrogen in the results, we have studied the influence of $^{15}N_2$ on the IR spectra of non-hydrogenated samples containing ~ 25-26 at. % nitrogen. The choice of this concentration is due to the structural changes occurring in the material above ~20 at. % nitrogen content.

Fig. 8 shows the ir spectra of two samples containing, $^{14}N_2$ (26.0 ± 0.5) at. % and $^{15}N_2$ (25.0± 0.5) at. %. The band associated to -C≡N (~2150 cm^{-1}) shifts $\Delta\omega \approx 35$ cm^{-1}, an amount compatible with the increasing reduced atomic mass and by assuming a constant oscillator strength.

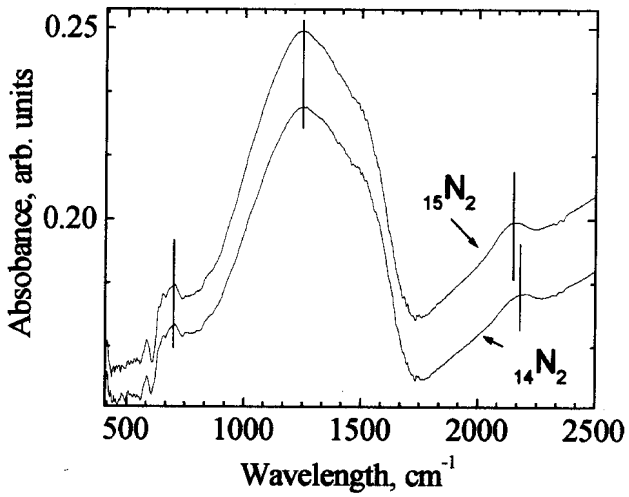

Figure 8. Infrared spectra of the a-C $^{15}N_x$ and a-C $^{14}N_x$ samples with 25 - 26 at. % nitrogen content. For the sake of clarity, the curves are shifted by a constant amount.

The region around 1000-1600 cm^{-1} is more complicated to analyze since only small changes are observed. This is due to the fact that the region contains a large contribution of vibration modes stemming from the sp^2 carbon skeletal structure. In the attempt to observed isotopic effects we have studied the difference spectrum of the samples (non-shown). The residual area under the main bands of the IR spectra is too small when compared with the area of the original bands. Furthermore, we have found that the spectra of two samples containing (26.0±0.5) at. % and (24.0±0.5) at. % respectively of $^{14}N_2$ can account for the residual area obtained in the difference spectrum.

V Discussion

The above data allowed us to draw a consistent picture of the structure of amorphous carbon nitride alloys prepared by IBAD. Additional information obtained from both the calculations and the experiments are discussed below.

In the theoretical study of random a-C1-xNx clusters, we calculated the enthalpy of formation (ΔH_f) of the alloy for different nitrogen concentrations. Fig. 9 (bottom) shows the quantity $[\Delta H_f(C_{n-x}N_x) - \Delta H_f(C_n)]/x$ as a function of the N concentration. Here, n is the total number of nitrogen and carbon atoms. ΔH_f represents the average energy necessary to incorporate one nitrogen atom either in the planar (curve a) or in the corrugated structures (curve b). The optimized geometry of both sets of clusters is very similar for low nitrogen concentrations, i.e., even full relaxation calculation results in a planar geometry. Buckling of the structure develops only above [N]/[C+N]~20%. These calculations show two important trends: 1) Both theoretical curves show a barrier for nitrogen incorporation at [N]/[N+C]~20%; and 2) above this threshold, the corrugated structure collapses to a state of much smaller energy than the planar structure.

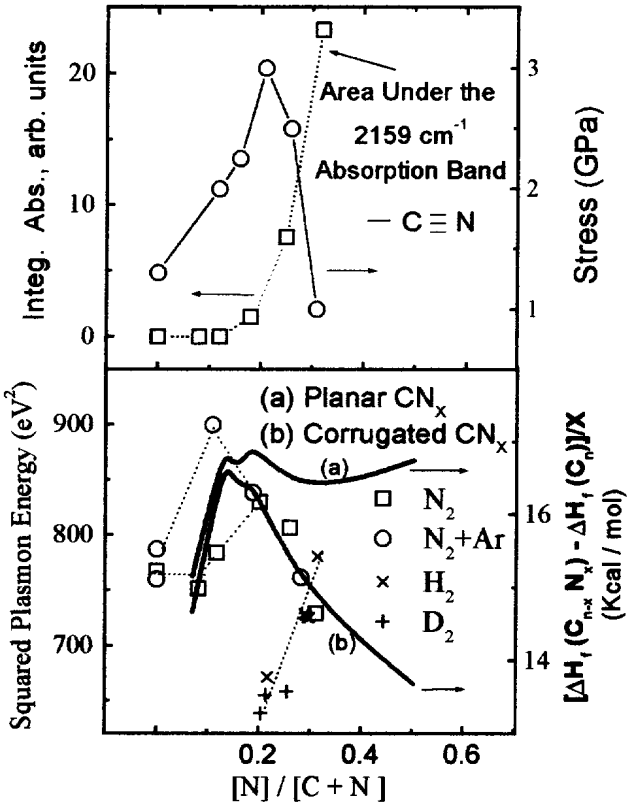

Figura 9. Bottom: plasmon energies for the studied samples vs. N concentration. The theoretical curves (solid) represent the difference in total enthalpies of formation between N substituted and non-substituted C clusters for planar (a) and corrugated (b) structures. Top: integrated intensity of the absorption band associated with -C≡N (cyano groups) vs. N. The gases used during the deposition are indicated. The dashed line is a guide to the eye.

In order to understand this behavior, we note that substitutional N in graphene sheets contributes two electrons to the graphite conduction band, which has an anti-bonding character. Therefore, the increase in N concentration will produce instabilities by the augmented electronic energy, distorting the system locally. Due to this, the hybridization of carbon and nitrogen change the character from sp2 to a sp3, localizing electrons in nitrogen lone-pairs. This is consistent with the fact that above ~20% [N]/[C] a band associated with localize lone-pair electrons emerge at the top of the valence band [11]. The plasmon energy $(\hbar\omega_m)^2$ associated to the C1s electron is a measure of the density of the material [26]. In Fig. 9 (bottom) we have plotted $(\hbar\omega_m)^2$ obtained from XPS spectra. [23]. The plasmon energy of the hydrogen free samples goes through a maximum around [N]/[C+N]~20%. Above [N]/[C+N]~20% the experimental data reasonably follow the "corrugated" theoretical enthalpy curve. This result suggests a spontaneous buckling of the structure, probably with the creation of dangling bonds and voids. Therefore, a decreasing density of the material is expected. Results from IR spectroscopy and stress support these conclusions.

The abrupt change in the plasmon energy is also accompanied by the emergence of a -C*equiv*N absorption band in the transmission IR spectra (not shown). The absorption characteristic of the -C≡N stretching mode (~2159 cm^{-1}) is incipient at [N]/[N+C]~ 20% indicating that only above this concentration cyano groups are formed (Fig. 9, top). This is probably induced by the existence of dangling bonds and voids, according to the theoretical simulation. The stress of the films as a function of the nitrogen content shows the same trend that the plasmon energy (Fig. 9, top). For low nitrogen concentration, the increasing stress is consistent with an increasing density of the material on nitrogen substitution of carbon. Above [N]/[N+C]~20%, the decreasing stress is a result of the buckling of the structure, i.e., a decreasing density of the material.

The plasmon energy of hydrogenated and deuterated samples increases monotonically in the range of studied compositions (cross and plus, Fig. 9, bottom). This result suggests that hydrogen promotes the formation of a soft, polymeric stress-free material with a quite small relative density. Furthermore, deuterated samples show the existence of primary amines. Finally, when exposed to air, the material incorporates hydroxyls by extensive hydrogen-bond formation [20].

The buckling of the otherwise planar carbon sheets upon nitrogen incorporation has another interesting consequence, which is the growing of closed molecular structures. These include heterofullerenes and nitrogen-doped nanotubes as well as other molecules yet to be characterized. We were able to build and optimize a molecular cage with composition $C_{24}N_{32}$ [7], a compound belonging to the to the C_3N_4 family, sketched in Fig. 10. This molecule has C_{4h} symmetry and its building blocks are eight-membered connected rings resembling the structure of β-C_3N_4. The nitrogen atoms are not all equivalent: eight of them have connectivity 3 and the remaining 24 nitrogens have connectivity 2.

The bonds around a connectivity 3 nitrogen are 1.47 Å to 1.48 Å in length and are not all in the same plane. Bond angles vary from 117° to 119°. Connectivity 2 atoms, on the other hand, show typical aromatic bonds of 1.36 Å and bond angle of 120°. All carbons are in equivalent sites, with all the bonds in the same plane. Computer calculations and experimental results suggest that other structures with different compositions are also possible. Preliminary results on soot production in a nitrogen atmosphere analyzed through mass spectroscopy measurements indicate the presence of species having mass/charge ratio (m/z) of 368, which is half the mass of $C_{24}N_{32}$. Assuming single ionization (z=1), this peak at m/z =368 correspond to a hypothetical molecule of mass equivalent to $4x(C_3N_4)$. Of course, assuming double ionization (z=2) this mass corresponds exactly to the mass of the ball displayed in Fig. 10. Furthermore, a set of species appear grouped around the ratio m/z=523 ("shrink-wrapping"). Starting in m/z=481 and up to 537, the peaks are sequentially obtained by adding the mass of one nitrogen atom. The sequence starting in m/z=552 is obtained adding to the 537 specie the masses of a nitrogen and a proton, the latest one probably stemming from residual water in the deposition chamber. Higher fullerenes are not present in the mass spectra suggesting that nitrogen substitution energetically favors smaller fullerenes. Experiments are currently being performed to produce and further characterize these heterofullerenes.

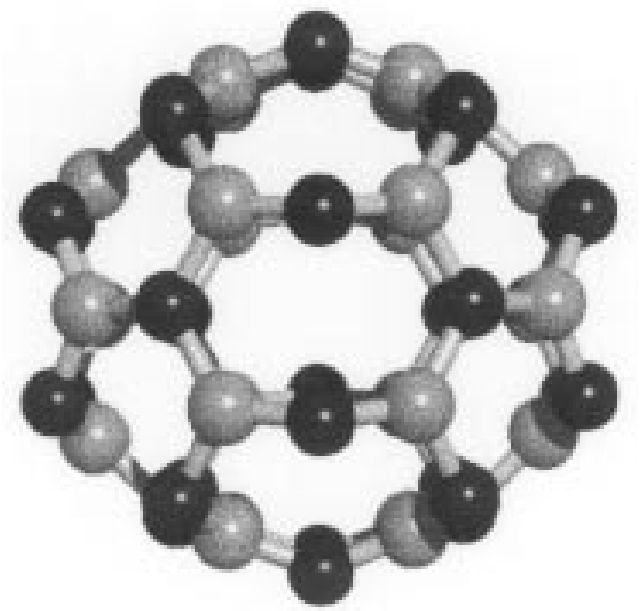

Figura 10. Ball-and-stick model of the molecular cage $(C_{24}N_{32}) = 8x(C_3N_4)$. C (gray) and N (black).

VI Conclusions

In summary, the electronic structure and vibrational spectra of CN_x films were experimentally determined by photoemission, Raman and IR spectroscopies. The spectra were compared and interpreted with results theoretically obtained on model molecules containing C and N atoms. The incorporation of N up to ∼20 at. % produces hard, dense and stressed material having a planar structure. Above this concentration, the extra electrons introduced by N destabilize the material and the structure curls and bends. A band the localized states arises at the top of the valence band, as in β-Si_3N_4. The introduction of hydrogen produces a hygroscopic, soft, and less dense material with polymeric characteristics. Numerical simulations show that several closed molecular structures are possible in hydrogen-free alloys containing more than 20 % at. N. In particular, a closed ball having the $8x(C_3N_4) = C_{24}N_{32}$ stoichiometry was theoretically predicted [7]. In order to test this possibility, the soot obtained vaporizing carbon in a arc discharge was studied by mass spectrometry. The mass spectra indicate, among other things, the presence of species having a mass compatible with the $4xC_3N_4$ stoichiometry (i.e., half of the atomic mass obtained by the numerical results). Of course, other combinations giving the same mass and different stoichimetry are also possible and more work is necessary to clearly identify the species present in the soot. Finally, attempts to concentrate the hypothetical $4xC_3N_4$ phase are under the way with the goal to use it as precursor for synthesizing the bulk crystalline β-C_3N_4 phase.

Acknowledgements

The authors are indebted to all the members of the Photovoltaic group and the Laboratory of Alternative Fuels, Unicamp, and to the Mass Spectroscopy Laboratory, Unicamp, for the mass spectra. This work was partially sponsored by Fapesp. The authors are CNPq fellows.

References

[1] For a recent review see E.G. Wang, Prog. Mat. Sci. **41**, 241 (1997).

[2] A. Liu and L. Cohen, Science **245**, 841 (1989).

[3] D. Marton, K. J. Boyd and J. W. Rabalais, Int. J. of Modern Phys. B, **9**, 3527 (1995), and references therein.

[4] P. Hammer, N. M. Victoria, and F. Alvarez, submitted, J. Vac. Technol. A (1999).

[5] H. Sjöström, S. Stasfsröm, M. Boman, and J.-E. Sundgren, Phys. Rev. B, **75**, 1336 (1995).

[6] N. Hellgren, M. P. Johansson, E. Broitman, L. Hultman, and J.E. Sundgren, Phys. Rev. B, **59**, 5162 (1999).

[7] M. C. dos Santos and F. Alvarez, Phys. Rev. B, **58**, 13918 (1998).

[8] K. Suenaga et al., Chem. Phys. Lett. **300**, 695 (1999).

[9] M. Terrones et al., Adv. Mater. **11**, 655 (1999).

[10] M.J.S. Dewar, E.G. Zoebish, E.F. Healy, J.J.P. Stewart, J. Am. Chem. Soc. **107**, 3902 (1985).

[11] S. Souto, M. Pickholz, M. C. dos Santos and F. Alvarez, Phys. Rev. B, **57**, 2536 (1998).

[12] For basis set definitions in Hartree-Fock calculations see, for instance, I.N. Levine in *Quantum Chemistry*, 3rd Edition, Allyn and Bacon, 1986.

[13] Y. Guo and W.A. Goddard III, Chem. Phys. Lett. **237**, 72 (1995).

[14] R. Lazzaroni, N. Sato, W.R. Salaneck, M.C. dos Santos, J.L. Brédas, B. Tooze, and D.T. Clark, Chem. Phys. Lett. **175**, 175 (1990), and references therein.

[15] F. Alvarez and M.C. dos Santos, J. Non-Cryst. Solids, in press.

[16] See, for instance, D. H. Parker, K. Chaterjjee, P. Wurz, K. R. Likke, M. J. Pellin, and L. M. Stock, in *The Fullerene*, Edited by: H. W. Kroto, J. E. Fisher, and D. E. Cox, Pergamon Press, Oxford, England, 1993.

[17] P. Hammer, N. M. Victoria, and F. Alvarez, J. Vac. Technol. A **16**, 2941 (1998).

[18] S. Souto and F. Alvarez, Appl. Phys. Lett. **70**, 1539 (1997).

[19] D. A. Shirley, Phys. Rev. B **5**, 4709 (1972).

[20] F. Alvarez, N. M. Victoria, P. Hammer, F. L. Freire Jr., and M. C. dos Santos, Appl. Phys. Lett. **73**, 1065 (1998).

[21] J.H. Kaufman, S. Metin, and D. D. Saperstein, Phys. Rev. B **39**, 13053 (1989).

[22] S. Souto and F. Alvarez, Appl. Phys. Lett. **70**, 1539 (1997).

[23] F. Alvarez, M.C. dos Santos, and P. Hammer, Appl. Phys. Lett. **73**, 3521 (1998).

[24] N. M. Victoria, P. Hammer, M.C. dos Santos, and F. Alvarez, Phys. Rev. B **61**, in press.

[25] J. Robertson, Prog. Solid St. Chem. **21**, 199 (1991)

[26] See, for instance, L. Ley in *Topics in Applied Physics, Vol 56: The physics of Hydrogenated Amorphous Silicon II.* Editor: J. D. Jonapoulos and G. Lucovsky, Springer-Verlag, Berlin, 1984, pag. 67.